Title

Traction forces mediated by integrin signaling are necessary for definitive endoderm specification

Journal

Journal of Cell Science, 128(10)

ISSN

0021-9533

Authors

Taylor-Weiner, Hermes
Ravi, Neeraja
Engler, Adam J

Publication Date

2015-05-15

DOI

10.1242/jcs.166157

Peer reviewed

© 2015. Published by The Company of Biologists Ltd | Journal of Cell Science (2015) 128, 1961-1968 doi:10.1242/jcs.166157

RESEARCH ARTICLE

Traction forces mediated by integrin signaling are necessary for definitive endoderm specification

Hermes Taylor-Weiner[1,2], Neeraja Ravi[1] and Adam J. Engler[1,2,3,*]

ABSTRACT

Pluripotent embryonic stem cells (ESCs) exert low-traction forces on their niche *in vitro* whereas specification to definitive endoderm *in vivo* coincides with force-mediated motility, suggesting a differentiation-mediated switch. However, the onset of contractility and extent to which force-mediated integrin signaling regulates fate choices is not understood. To address the requirement of tractions forces for differentiation, we examined mouse embryonic stem cell (ESC) specification towards definitive endoderm on fibrillar fibronectin containing a deformation-sensitive FRET probe. Inhibiting contractility resulted in an increase in the observed fibronectin FRET intensity ratio but also decreased the amount of phosphorylated nuclear SMAD2, leading to reduced expression of the definitive endoderm marker SOX17. By contrast ESCs maintained in pluripotency medium did not exert significant tractions against the fibronectin matrix. When laminin-111 was added to fibrillar matrices to improve the efficiency of definitive endoderm induction, ESCs decreased their fibronectin traction forces in a laminin-dependent manner; blocking the laminin-binding α3-integrin restored fibronectin matrix deformation and reduced SOX17 expression and SMAD2 phosphorylation, probably because of compensation of inhibitory signaling from SMAD7 after 5 days in culture. These data imply that traction forces and integrin signaling are important regulators of early fate decisions in ESCs.

KEY WORDS: Endoderm, Embryonic stem cells, Integrin signaling, Extracellular matrix, SMAD

INTRODUCTION

Early in development, embryonic stem cells (ESCs) migrate and form the definitive endoderm layer of trilaminar embryos. Such morphogenetic events require traction-force-mediated cell migration and signaling from extracellular matrix (ECM) proteins, especially fibronectin (FN) (Darribère and Schwarzbauer, 2000; Keller, 2005; Skoglund et al., 2008). Apart from facilitating cell movement, the ECM is also likely a cue for directing cell fate given that ESCs and progenitor cells are known to respond to a variety of matrix-associated signals, which are presented in precise spatial and temporal patterns during development (D'Amour et al., 2005; Higuchi et al., 2010; Murry and Keller, 2008). For example, mouse ESCs maintain pluripotency when cultured on soft ECM because they cannot exert significant contractile forces against the ECM (Chowdhury et al., 2010a), but upon application of external forces, ESCs lose pluripotency (Chowdhury et al., 2010b). In concert with matrix forces, matrix composition also drives specification as FN localizes to mouse endoderm (Wartiovaara et al., 1978) and laminin-containing basement membrane forms between primitive ectoderm and endoderm layers (Li et al., 2003). In fact, β1-integrin is required for endoderm differentiation (Liu et al., 2009) and its knockout results in embryonic lethality (Sheppard, 2000). Taken together, this evidence highlights physical and biochemical regulation of early development by the ECM, as well as its potential to guide ESC differentiation. Yet despite such evidence, protocols directing ESC differentiation have focused almost exclusively on soluble signaling. For example, activin A, a TGF-β family protein, and Wnt3a are commonly added to ESC cultures to induce differentiation to definitive endoderm (D'Amour et al., 2005; Yasunaga et al., 2005). These soluble factor differentiation strategies likely benefit indirectly from ECM signaling given that these signals direct ESCs to assemble lineage-specific ECM; for example, activin A induces ESC assembly of FN and laminin-111 (Taylor-Weiner et al., 2013).

Despite these efforts in understanding both growth factor and ECM signaling, feedback mechanisms between soluble signals and matrix signaling are still poorly understood, especially those involving physical stimuli such as contractility. Therefore, we sought to understand how the soluble factors commonly used to direct definitive endoderm differentiation induce biophysical and biochemical changes in ESCs and their associated matrix. To do this, we employed a force-sensitive FN matrix assay and examined whether the ECM changes induced by the soluble signals contributed to definitive endoderm differentiation. Taken together, these data draw attention to the supportive feedback between soluble factor and matrix signaling and implicate ECM as a potential new modulator of ESC fate.

RESULTS

Traction force inhibition prevents definitive endoderm specification

Undifferentiated ESCs exert low-traction forces (Chowdhury et al., 2010a) but switch to a highly contractile state in order to migrate and differentiate into definitive endoderm during gastrulation (Keller, 2005; Skoglund et al., 2008); these data suggest contraction occurs concurrently with differentiation and might contribute to lineage commitment signals. To examine whether traction forces are required for definitive endoderm differentiation, mouse ESCs (CCEs and R1 lines) were grown on decellularized fibroblast-derived ECMs (Chen et al., 1978). After 5 days of definitive endoderm induction, the ESCs expressed the definitive endoderm transcription factor marker SOX17 (Fig. 1A, left). However the addition of 10 μM blebbistatin, a non-muscle myosin II inhibitor, each day to the definitive endoderm induction medium reduced SOX17 expression by fourfold (Fig. 1A, right), based on nuclear staining intensity (Fig. 1B). These data suggest that inhibition of traction forces is sufficient to prevent ESCs from undergoing definitive endoderm differentiation in response to soluble signals.

[1]Department of Bioengineering, University of California, San Diego, La Jolla, CA 92093, USA. [2]Sanford Consortium for Regenerative Medicine, La Jolla, CA 92037, USA. [3]Biomedical Sciences Program, University of California, San Diego, La Jolla, CA 92093, USA.

*Author for correspondence (aengler@ucsd.edu)

Received 14 November 2014; Accepted 24 March 2015

Journal of Cell Science (2015) 128, 1961-1968 doi:10.1242/jcs.166157

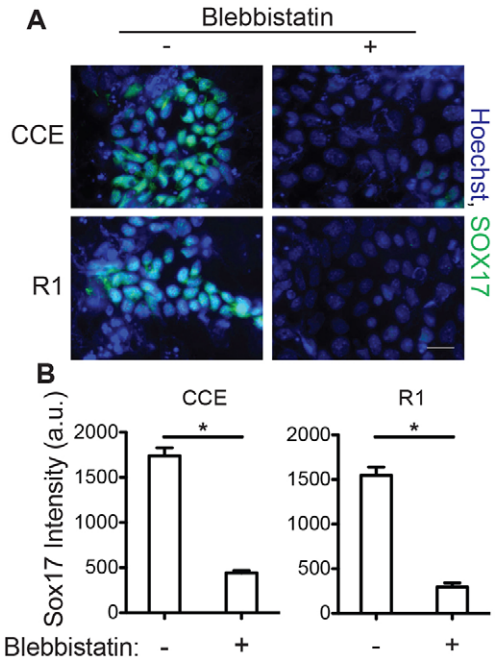

Fig. 1. Traction forces are necessary for definitive endoderm specification. Mouse ESCs (CCE and R1) were grown on decellularized fibroblast-derived ECM in definitive endoderm induction medium, with or without 10 µM blebbistatin. (A) Immunofluorescent images of SOX17 (green) and Hoechst 33342 (blue)-stained nuclei were taken after 5 days and (B) the mean±s.e.m. (n>300) nuclear intensity of SOX17 was quantified. *P<0.05. Scale bar: 20 µm. a.u., arbitrary units.

Traction forces are activated during differentiation and transiently regulate TGF-β signaling

To evaluate whether definitive endoderm induction medium activates traction forces, FN matrix strain was monitored in decellularized fibroblast-derived ECM using a FN force-sensitive Förster resonance energy transfer (FRET) probe (FRET-FN) (Baneyx et al., 2001; Smith et al., 2007) where matrix strain is related to the FRET intensity ratio, that is, the ratio of acceptor to donor fluorophore intensity. To ensure the FRET ratio was sensitive to FN unfolding, the FRET-FN probe was characterized in the chemical denaturant guanidine hydrochloride (GdnHcl) (supplementary material Fig. S1A). The ratio of acceptor to donor peak emission decreased twofold over a 4 M change in GdnHCl (supplementary material Fig. S1B), indicating that the FRET-FN was sensitive to chemical denaturation. Fibroblasts grown in medium containing FRET-FN assembled the probe into the ECM (supplementary material Fig. S1C, right), allowing measurements of matrix strain. Upon decellularization, the average FRET-FN intensity ratio increased (supplementary material Fig. S1C, left), showing that the matrix was responsive to the removal of fibroblast forces and was suitable for monitoring ESC contractility.

To determine whether ESCs exert traction forces during pluripotency or definitive endoderm induction, ESCs (CCE and R1 lines) were grown on decellularized FRET-FN matrices. During 5 days of definitive endoderm or pluripotency induction, ESCs remodeled the matrix, affecting both its overall structure and its FRET intensity ratio (Fig. 2A). ESCs in definitive endoderm induction medium assembled a thin fibrillar matrix, whereas R1s and CCEs in pluripotency medium assembled thick FN fibers and punctate FN, respectively (Fig. 2A). Moreover, the FRET intensity ratio of the matrix in the definitive endoderm condition was lower than in the pluripotency-inducing condition or in the decellularized control (Fig. 2B), suggesting that the FN matrix was exposed to greater strain during definitive endoderm induction. Although these data indicate that definitive endoderm induction causes ESCs to impart strain onto their matrix, they do not show whether the strain results from changes in ECM organization or from active cell traction forces. To address this, ESCs were grown on FRET-FN matrices for 5 days and then treated with 50 µM blebbistatin for 1 h to inhibit active cell contractility. The cessation of traction forces reduced or eliminated differences in matrix strain between pluripotency and definitive endoderm cultures (Fig. 2C). Importantly, a 1-h blebbistatin treatment did not affect *Sox17* gene expression in comparison to untreated ESCs (Fig. 2D). Taken together, these data suggest that traction forces are initially inhibited in the unspecified ESC state, but become activated upon definitive endoderm differentiation.

Although we have shown that definitive endoderm induction mediated by growth factors increases the ESC traction forces, it is not clear whether traction forces feedback on soluble factor signaling. Activin A is necessary for definitive endoderm induction (D'Amour et al., 2005) and acts by stimulating the TGF-β signaling pathway mediated by SMAD2, SMAD3 and SMAD4. Consistent with this evidence, R1 ESCs treated with definitive endoderm induction medium on decellularized ECM expressed phosphorylated SMAD2 (phospho-SMAD2) (supplementary material Fig. S2 and Fig. S3A, cell lysate) and activated contractility (supplementary material Fig. S3) after 2 days. However, when traction forces were inhibited by a daily addition of 10 µM blebbistatin, we did not observe changes in the association of phospho-SMAD2 and SMAD4 (Fig. 3A, SMAD4 IP). Instead, we observed a 30% reduction in nuclear phospho-SMAD2 after 2 days but not after 5 days (Fig. 3B,C). R1 ESCs in definitive endoderm medium supplemented with 10 µM blebbistatin from day 0 to day 2 of culture exhibited decreased SOX17 expression, whereas those treated with blebbistatin from day 3 to day 5 did not exhibit impaired differentiation (Fig. 3D). These data imply that blebbistatin inhibits activin-A-induced TGF-β signaling by preventing the initial nuclear translocation of phospho-SMAD2 and that 2 days of phospho-SMAD2 signaling is sufficient for SOX17 expression. These results suggest that alternative blebbistatin-insensitive signaling pathways might become activated after 2 days of definitive endoderm induction.

ECM signaling regulates definitive endoderm induction and contractility

Although FN matrix is necessary for differentiation (Darribère and Schwarzbauer, 2000), recent reports have suggested that specific laminin isoforms also promote definitive endoderm differentiation (Higuchi et al., 2010; Taylor-Weiner et al., 2013). To understand how traction forces augment differentiation in more complex ECM, ESCs were cultured on decellularized ECM where exogenous laminin had been previously added to fibroblast medium to create laminin-111- and FN-rich matrix. Consistent with these reports, laminin-111 was detected in the matrices without exogenous laminin after 5 days of ESC culture, indicating that ESCs produce laminin-111. However, the presence of laminin from the outset enhanced the final laminin-111 concentration (Fig. 4A). These data suggest that temporal changes in blebbistatin sensitivity (Fig. 3C,D) might be due, in part, to changes in ECM composition created by endogenous expression of laminin-111.

We next cultured R1 ESCs with a function-blocking anti-α5β1-integrin antibody on FRET-FN ECM containing laminin so as to inhibit FN signaling. After 5 days of definitive endoderm induction, R1 ESCs exhibited a laminin-dependent increase in nuclear SOX17 staining in agreement with previous findings (Higuchi et al., 2010;

Journal of Cell Science (2015) 128, 1961-1968 doi:10.1242/jcs.166157

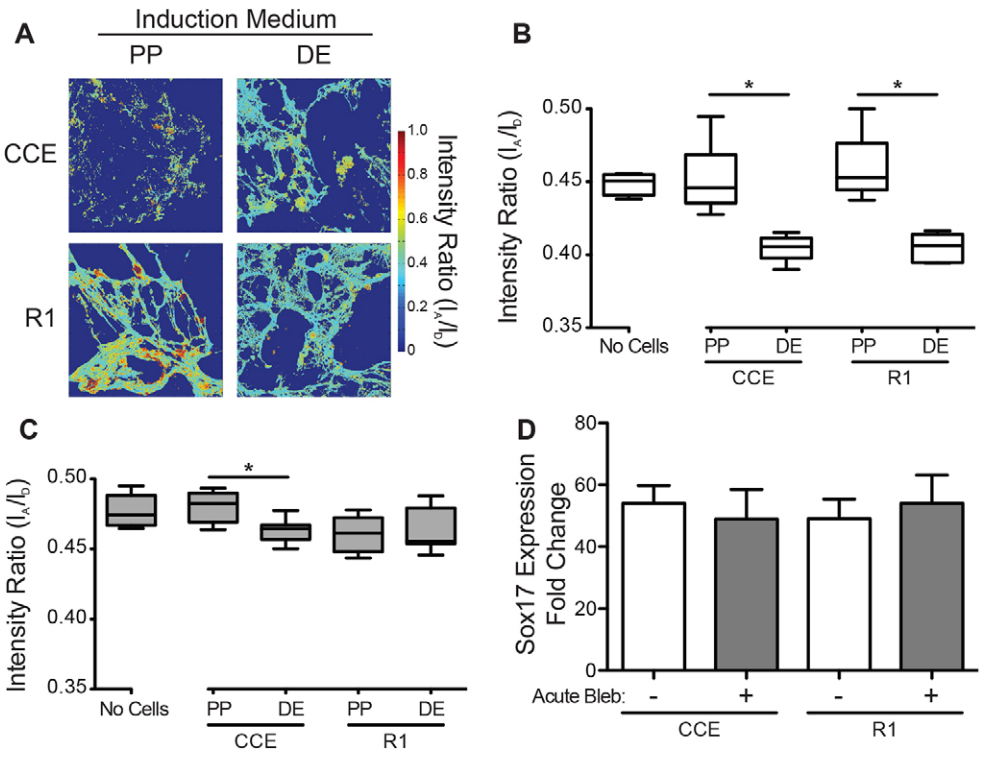

Fig. 2. Cell contractility is activated upon definitive endoderm induction. Mouse ESCs (CCE and R1) were grown in either definitive endoderm (DE) or pluripotency (PP) induction medium on decellularized fibroblast-derived ECM containing FRET-FN. (A) Confocal *z*-stacks of the FRET fibronectin matrix were captured after 0 (No Cells) and 5 days of induction and (B) the average FRET intensity ratio of the ESC associated matrix was quantified (n>16). ESCs were treated with 50 µM blebbistatin for 1 h at the end of definitive endoderm or pluripotency induction and (C) the average FRET intensity ratios of ESC-associated matrix (n>16) and (D) SOX17 gene expression were quantified (mean±s.e.m., n=3). For boxplots, the box represents the 25–75th percentiles, and the median is indicated. The whiskers show the 10–90th percentiles. *P<0.05.

Taylor-Weiner et al., 2013); α5β1-integrin inhibition reduced SOX17 expression independently of laminin (Fig. 4B). However, the FRET-FN intensity ratio was significantly higher for ESCs cultured on laminin-containing matrices, indicating that there was a reduction in FN matrix strain (Fig. 4C). These data suggest that α5β1-integrin signaling enhances definitive endoderm differentiation but that definitive endoderm cells preferentially bind laminin. Given that the FRET sensor is only on FN, an integrin-binding switch would result in an increase in FRET ratio. Although these data suggest preferential laminin binding, they do not show whether this is specific to definitive endoderm. To address this, ESCs were cultured on FRET-FN ECM with exogenous laminin. The laminin-dependent increase in FRET intensity ratio was observed in definitive endoderm induction medium but not in pluripotency conditions (Fig. 5). However, unspecified ESCs might exert low-traction forces even in the absence of laminin and so any laminin-induced reduction in FN matrix strain would be difficult to observe.

Laminin regulates differentiation and contractility through α3β1-integrin

To understand how ESCs sense laminin, we examined whether function-blocking antibodies for the laminin-binding integrins α6-integrin [GoH3 antibody (Aumailley et al., 1990)] and α3-integrin [Ralph 3.1 (DeFreitas et al., 1995; Demyanenko et al., 2004)] would affect definitive endoderm differentiation and contractility. Inhibition of α3-integrin, either alone or with α6-integrin inhibition, reduced nuclear SOX17 expression fourfold (Fig. 6A). Blocking α3-integrin or both α3- and α6-integrin caused a decrease in the FRET-FN intensity ratio, indicating greater FN matrix strain and a shift in α5β1-integrin binding (Fig. 6B). By contrast, inhibition of the α6-integrin did not significantly alter SOX17 staining and had no effect on FN matrix strain (Fig. 6A,B). Taken together, these data indicate that definitive endoderm cells primarily sense laminin through α3- but not α6-integrin, and that its inhibition redistributes tractions from laminin to FN. Although these data suggest that α6-integrin inhibition does not prevent laminin sensing, it does not capture whether integrin expression changes occur when laminin-binding integrins are blocked. To address this, the relative α6- and α3-integrin expression on R1 ESCs was examined by fluorescence-activated cell sorting (FACS) during blocking. Inhibiting α6-integrin increased expression of α3-integrin by 70% whereas α3-integrin inhibition did not affect the expression of α6-integrin (supplementary material Fig. S4A). These data suggest that the lack of response to the antibody blocking α6-integrin function might be due in part to compensatory mechanisms that cause increased expression of α3-integrin.

Given that tractions regulated TGF-β signaling and inhibition of α3-integrin shifted traction forces from laminin to FN, we next examined the extent that α3-integrin influenced TGF-β signaling in differentiating R1 ESCs. Loss of α3-integrin increases expression of the TGF-β inhibitor SMAD7 (Nakao et al., 1997; Reynolds et al., 2008), and so α3-integrin was inhibited in differentiating R1 ESCs on matrices with exogenous laminin. α3-integrin inhibition increased SMAD7 and decreased phospho-SMAD2 levels after 5 days but not after 2 days (Fig. 6C). These data suggest that α3-integrin signaling might prevent accumulation of SMAD7, a TGF-β pathway inhibitor, which is expressed in response to prolonged activin A treatment. R1 ESCs treated with 10 µM blebbistatin on laminin-containing ECM for 5 days showed inhibited SOX17 expression (Fig. 6D), but did not show altered levels of SMAD7 or phospho-SMAD2 (Fig. 6E). Taken together, these data indicate that cell traction forces and α3-integrin promote definitive endoderm differentiation through independent mechanisms that enhance activin-A-mediated TGF-β signaling.

DISCUSSION

Data presented here examined how soluble signals, such as activin A and Wnt3a, that induce definitive endoderm specification regulate

Journal of Cell Science

Journal of Cell Science (2015) 128, 1961-1968 doi:10.1242/jcs.166157

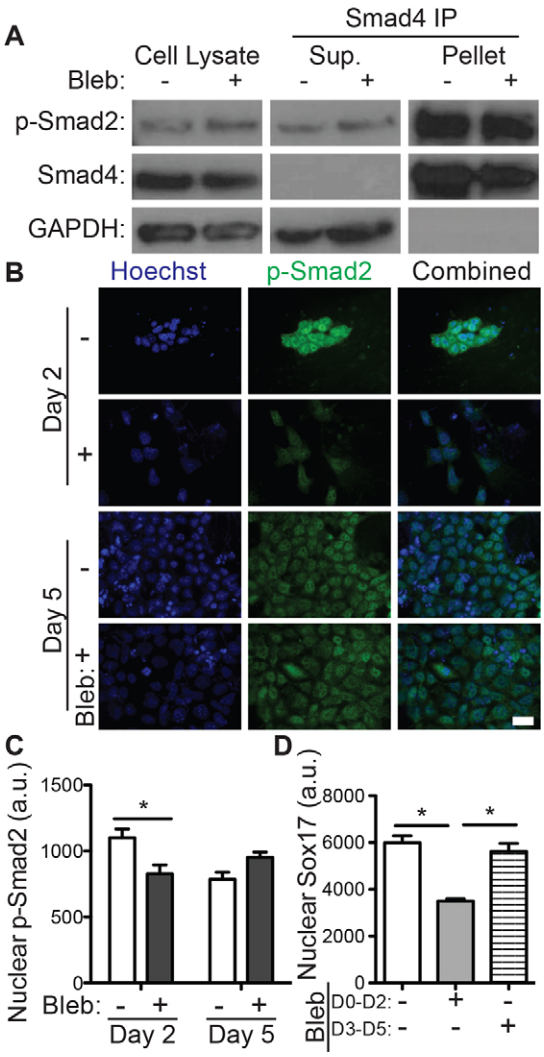

Fig. 3. Disruption of traction forces inhibits TGF-β signaling. R1 ESCs were grown on decellularized fibroblast-derived extracellular matrix in definitive endoderm induction medium with or without 10 µM blebbistatin. (A) Blots show cells that were lysed after 2 days (left) as well as the supernatant (Sup., center) and pulldown (pellet, right) fractions of SMAD4 immunoprecipitation (IP). Blots are shown for phospho-SMAD2 (p-SMAD2), SMAD4 and GAPDH. (B) Immunofluorescent images of phospho-SMAD2 (green) and Hoechst 33342 (blue)-stained nuclei taken after 2 and 5 days are shown along with (C) quantification of the mean±s.e.m. (n>200) nuclear intensity of phospho-SMAD2. (D) Immunofluorescent images of SOX17 and Hoechst-stained nuclei were quantified (mean±s.e.m., n>1000) after 5 days of the indicated blebbistatin treatment. *P<0.05. Scale bar: 20 µm. a.u., arbitrary units.

biophysical changes in ESCs and their associated ECM. Definitive endoderm induction activated cell tractions (Fig. 7, center) and caused sensitivity to extracellular laminin. Both these changes were supportive of TGF-β signaling, which was necessary to achieve optimal definitive endoderm induction. These data support a signaling model where the induction of definitive endoderm depends on the force-sensitive localization of phospho-SMAD2 (Fig. 7, left), which is regulated in parallel by laminin-sensitive SMAD7 inhibition of SMAD2 phosphorylation (Fig. 7, right).

Traction-sensitive differentiation

Consistent with the results from ESCs on synthetic hydrogels with passive (Chowdhury et al., 2010a) or actively applied forces (Chowdhury et al., 2010b), these results indicate that in order to differentiate, ESCs must transition from a low-traction pluripotent state to a primed state with active cell-matrix contractility. Using deformation-sensitive FRET-FN matrices (Smith et al., 2007), we found that the force-sensitive phenotype changes in ESCs appear to be consistent with the epithelial–mesenchymal transition (EMT) that ESCs undergo during gastrulation where forces increase to allow motility (Thiery and Sleeman, 2006). Although inhibition of traction force maintains pluripotency (Chowdhury et al., 2010a), these data present the first demonstration that traction force activation is required for definitive endoderm differentiation on a fibrillar ECM. Taken together with EMT observations, these data suggest a more general role for traction-mediated loss of pluripotency on fibrillar matrix.

Specifically for the transition from ESCs to definitive endoderm, we found that inhibiting tractions prevented definitive endoderm marker expression in response to activin A by interfering with nuclear accumulation of phospho-SMAD2 (Fig. 7, left). Given that TGF-β and Wnt signaling are known promoters of EMT (Kemler et al., 2004; Thiery and Sleeman, 2006), this result suggests that regulatory feedback mechanisms similar to those that occur during EMT, for example the activation of tractions, promote the signaling pathways that initiate transition. These data add TGF-β signaling to a growing list of signaling pathways [e.g. Src signaling (Na et al., 2008), Src-independent Rac activation (Poh et al., 2009)] that are regulated by a combination of mechanical and chemical cues (Li et al., 2011). However, it is still unclear whether other early embryonic lineages that undergo EMT and activate traction forces (Thiery and Sleeman, 2006) also use similar protein phosphorylation and nuclear translocation mechanisms to direct cell fate. Several other mechanosensitive signaling mechanisms have been proposed including Rho-ROCK, stretch-activated channels and force-induced conformational changes (Holle and Engler, 2011), and all of these methods could induce changes that are similar to what was observed here. In fact, it is known that adult stem cells are force sensitive (Guvendiren and Burdick, 2012), as with ESCs here, but use nuclear-based (Pajerowski et al., 2007; Swift et al., 2013) and focal-adhesion-based sensors (Holle et al., 2013). These data argue that there is a need for careful specific observations for each stem cell type rather than more general characterizations.

Laminin modulation of contractile signaling

Integrin-specific traction force activation during definitive endoderm differentiation suggests that ESCs might sense the properties of their ECM using forces transmitted through integrins. Indeed, we and others have shown that the ECM proteins fibronectin and laminin positively regulate definitive endoderm induction (Higuchi et al., 2010; Taylor-Weiner et al., 2013). Here, we show that laminin modulates integrin adhesions and tractions separately from FN, possibly due to preferential binding. More specifically, data has suggested that the laminin-binding α3β1-integrin can act as a trans-dominant inhibitor of FN- and collagen-binding integrins (Hodivala-Dilke et al., 1998). Indeed, we found that inhibition of α3β1-integrin increased FN matrix strain and reversed the laminin-dependent improvement in definitive endoderm differentiation. However, underlying these changes are observations that α3-integrin loss leads to increased SMAD7 expression, which is an inhibitor of the TGF-β pathway (Nakao et al., 1997; Reynolds et al., 2008). We found that inhibition of α3-integrin increased the SMAD7 expression in ESCs and disrupted their ability to differentiate into definitive endoderm through SMAD7-mediated inhibition of activin A signaling. This then interfered with traction-

Journal of Cell Science (2015) 128, 1961-1968 doi:10.1242/jcs.166157

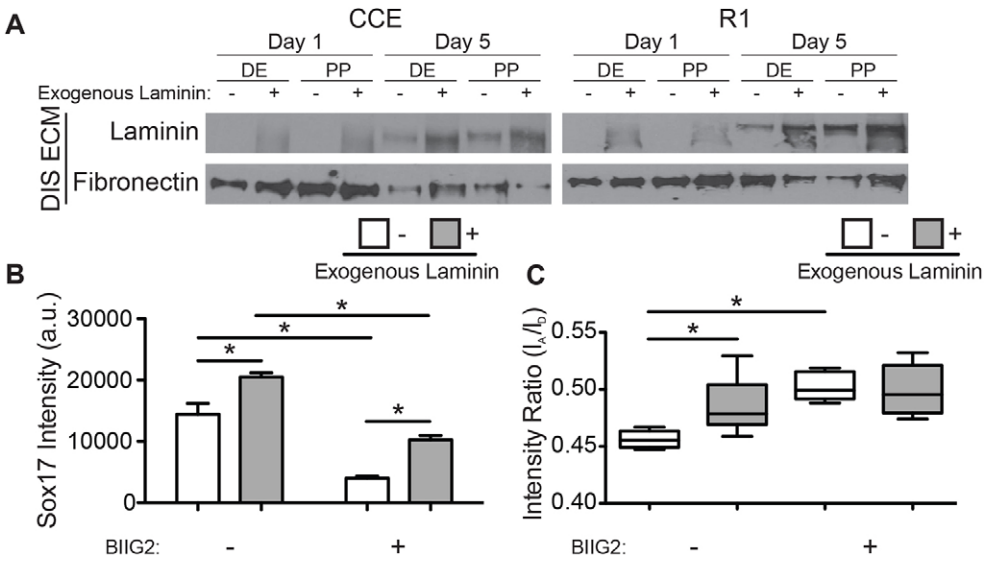

Fig. 4. ECM signaling regulates definitive endoderm induction and contractility. (A) Mouse ESCs (CCE and R1) were grown in definitive endoderm (DE) or pluripotency (PP) induction medium on decellularized fibroblast-derived matrices supplemented with FRET fibronectin and either 0 µg/ml (– exogenous laminin) or 50 µg/ml (+ exogenous laminin) mouse laminin-111. Equal amounts of DOC-insoluble ECM were blotted for laminin or fibronectin after 1 and 5 days of ESC culture. (B) R1 ESC mean±s.e.m. (n>300) nuclear SOX17 staining intensity and (C) average extracellular matrix FRET intensity ratios (the box represents the 25–75th percentiles, and the median is indicated; the whiskers show the 10–90th percentiles, n>10) were measured after 5 days of definitive endoderm induction in the presence or absence of the α5β1-integrin function-blocking antibody BIIG2. *P<0.05. a.u., arbitrary units.

mediated phosphorylation and translocation of SMAD2 (Fig. 7, right). Other integrin-associated proteins, such as kindlin and integrin-linked kinase, have been proposed as regulators of TGF-β signaling (Boo and Dagnino, 2013; Rognoni et al., 2014), suggesting that parallel integrin signaling pathways could also be regulating definitive endoderm induction. Taken together, these results suggest that integrin signaling might regulate soluble signaling pathways throughout development and could be an important tool for directing ESC differentiation.

The findings that traction forces and ECM proteins can regulate growth factor signaling is consistent with reports that stem cell fate can be directed by cell tractions (Fu et al., 2010; Khetan et al., 2013) and ECM properties, including stiffness (Wen et al., 2014; Young and Engler, 2011) and ligand composition (Brafman et al., 2013; DeQuach et al., 2011). Taken together, these results demonstrate that ECM signaling and soluble factor signaling can be co-regulated and that the properties of culture substrates should be carefully considered when designing ESC differentiation protocols.

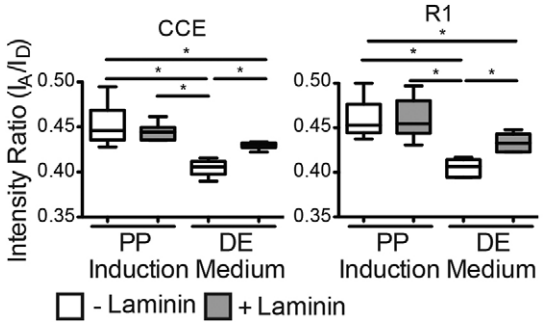

Fig. 5. Laminin effects on contractility are specific to definitive endoderm. After 5 days in either definitive endoderm (DE) or pluripotency (PP) induction medium, and the average FRET intensity ratios of ESC-associated matrix were quantified (the box represents the 25–75th percentiles, and the median is indicated; the whiskers show the 10–90th percentiles) for mouse ESCs (CCE and R1) grown on decellularized fibroblast-derived ECM containing FRET-FN and either 0 µg/ml (– laminin) or 50 µg/ml (+ laminin) exogenous laminin. n>16. *P<0.05.

MATERIALS AND METHODS

Cell culture

All cell types were cultured at 37°C in an incubator containing 5% CO_2. Mouse ESCs [CCE cell line, Stem Cell Technologies (Robertson et al., 1986); R1 cell line, American Type Culture Collection (Nagy et al., 1993)] were maintained on gelatin-coated substrates in Dulbecco's modified Eagle's medium (DMEM) supplemented with 2 mM L-glutamine, 1 mM sodium pyruvate, 50 U/ml penicillin, 50 µg/ml streptomycin, 1 mM non-essential amino acids, 15% fetal bovine serum screened for mouse ESCs (Thermo Scientific), 100 µM 1-thioglycerol and 10^3 U/ml leukemia inhibitory factor. Mouse ESCs were passaged as single cells upon reaching 80% confluence, about every 2 days, to maintain their pluripotent state. Mouse fibroblasts (NIH-3T3) were grown in DMEM containing 10% bovine calf serum (Thermo Scientific), 4 mM L-glutamine, 1 mM sodium pyruvate, 100 U/ml penicillin, 100 µg/ml streptomycin and 0.25 µg/mL amphotericin B.

To induce definitive endoderm differentiation, ESCs (CCEs and R1s) were seeded as single cells at a density of 10^4 cells/cm^2 in definitive endoderm induction medium composed of 1:1 Iscove's modified Dulbecco's medium and Ham's F-12 nutrient mixture, and 1% fetal clone II serum (Thermo Scientific), 2 mM L-glutamine, 50 U/ml penicillin, 50 µg/ml streptomycin, 0.1% BSA, 450 µM 1-thioglycerol, 100 ng/ml activin A and 10 ng/ml Wnt3a. The non-muscle myosin II inhibitor, blebbistatin, was added to cultures at the indicated concentration to disrupt myosin activity and thereby inhibit ESC traction stresses.

Integrin-blocking antibodies

To disrupt specific integrin–ECM interactions, the following function-blocking antibodies were added to differentiation cultures: 10 µg/ml of GoH3 α6-integrin function-blocking antibody (Beckman Coulter), 5 µg/ml of Ralph 3.1 α3-integrin function-blocking antibody (Developmental Hybridoma Bank, Iowa City, IA), 6 µg/ml of BIIG2 α5-integrin function-blocking antibody (Developmental Hybridoma Bank, Iowa City, IA) or 50 µg/ml of a control rabbit IgG antibody. In addition to including blocking antibodies in differentiation medium during culture (which was replenished every 1–2 days), ESCs in suspension were also incubated in differentiation medium containing the antibody at 37°C for 1 h prior to seeding.

Journal of Cell Science (2015) 128, 1961-1968 doi:10.1242/jcs.166157

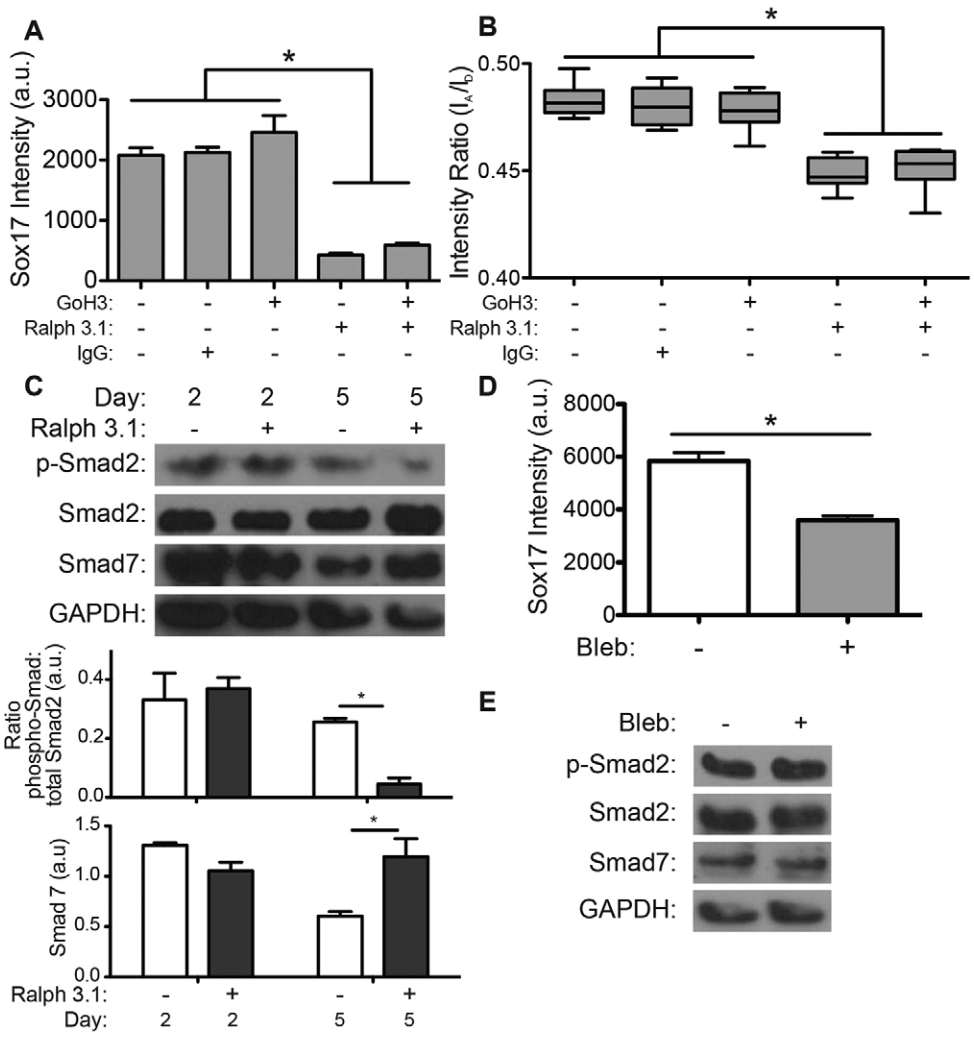

Fig. 6. Laminin-containing ECM affects FRET-FN contractility and definitive endoderm induction through α3-integrin-mediated signaling. R1 ESCs were grown on decellularized fibroblast-derived ECM with FRET-FN and 50 µg/ml exogenous mouse laminin. (A) Nuclear SOX17 staining intensity was quantified (mean±s.e.m., n>500) after 5 days for ESCs in definitive endoderm induction medium containing the indicated integrin function-blocking antibodies. (B) FRET intensity ratios of ESC-associated matrix was quantified after 5 days for R1 ESCs in the indicated culture conditions. The box represents the 25–75th percentiles, and the median is indicated; the whiskers show the 10–90th percentiles; n>10. (C) Cells were lysed after 2 and 5 days and equal amounts of cell lysis were separated by SDS-PAGE and blotted with phospho-SMAD2, SMAD2, SMAD7 and GAPDH antibodies. The relative levels (mean±s.e.m., n=3) are shown in the graph below the blot. (D) Nuclear SOX17 staining intensity was quantified (mean±s.e.m., n>500) after 5 days of definitive endoderm induction with (+) or without (–) 10 µM blebbistatin. (E) Cells were lysed after 5 days and blotted with antibodies against phospho-SMAD2, SMAD2, SMAD7 and GAPDH. *P<0.05.

Preparation of FRET-FN

FN was isolated from human plasma using gelatin–sepharose binding and eluted with 6 M urea. Isolated FN was concentrated to ∼3 mg/ml using an Amicon Ultra Centrifugal Filter (10 kDa NMWL; Millipore), according to manufacturer's instructions, and denatured for 15 min in 4 M guanidine hydrochloride (GdnHCl). Denatured FN was dual-labeled with Alexa Fluor 488 (donor) and Alexa Fluor 546 (acceptor) fluorophores, as previously described (Baneyx et al., 2001; Wen et al., 2014). Briefly, denatured FN was incubated with a 30-fold molar excess of Alexa Fluor 546 C5 Maleimide (Life Technologies) for 2 h to label cysteine residues within the III_7 and III_{15} domains of FN. The single-labeled FN was buffer exchanged into 0.1 M sodium bicarbonate pH 8.3 and separated from unreacted Alexa Fluor 546 fluorophores using a spin desalting column (Thermo Scientific), according to the manufacturer's instructions. The single-labeled FN was

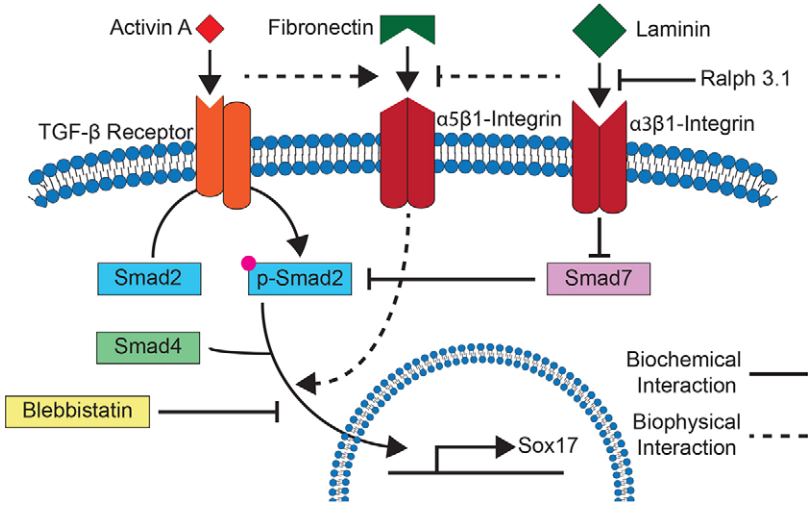

Fig. 7. Model for α3-integrin and traction force signaling during definitive endoderm differentiation. During definitive endoderm differentiation, activin A binds to TGF-β receptors, resulting in the activation of α5β1-integrin-mediated contractility and phosphorylation of SMAD2 and SMAD3. SMAD7, a competitive inhibitor of SMAD2 and SMAD3 phosphorylation, and α5β1-integrin are inhibited by α3β1-integrin-mediated laminin sensing. Treatment with blebbistatin, an inhibitor of myosin activity and therefore traction forces, prevents accumulation of the SMAD2–SMAD3–SMAD4 complex within the nucleus.

then incubated with a 40-fold molar excess of Alexa Fluor 488 succinimidyl ester (Life Technologies) for 1 h to label amine residues. Unreacted Alexa Fluor 488 fluorophores were removed using a spin desalting column and dual-labeled FN was stored with 10% glycerol at −20°C. The average number of acceptor and donor fluorophores per FN were determined using published extinction coefficients and the absorbance of the dual-labeled FN at 280, 498 and 556 nm. FRET-FN was prepared in two batches with an average of 8.8 donors and 3.2 acceptors (Figs 2, 5; supplementary material Fig. S1) and 7.3 donors and 3.3 acceptors (Figs 4, 6) per FN dimer.

The emission spectrum of the dual-labeled FN was characterized in varying concentrations of denaturant by fluorescence spectroscopy using a Synergy 4 Microplate Reader (BioTek). Briefly, 100 µg/ml dual-labeled FN in PBS was denatured in 0 to 4 M guanidine hydrochloride (GdnHcl) and excited at 484 nm. The resulting emission spectrum was measured from 510 to 700 nm (supplementary material Fig. S1A) and the ratio of the maximum acceptor emission (~570 nm) to the maximum donor emission (~520 nm) was determined at each concentration of GdnHcl (supplementary material Fig. S1B).

Analysis of FRET-FN images

Images of the dual-labeled FN were acquired on a Zeiss LSM 780 Confocal Microscope and analyzed using a custom MATLAB script, as previously described (Smith et al., 2007). Briefly, images were averaged with a 3×3 pixel sliding block and pericellular regions of DAPI-stained cells were manually selected for analysis. The FRET ratio for each pixel within a selected region was calculated by dividing the intensity of that pixel in the acceptor image by its corresponding intensity in the donor image. FRET ratios less than 0.05 and greater than 1.0 were excluded from analysis. The mean FRET ratio within the selected regions was calculated for each group of cells and then averaged over all the groups in each condition.

Preparation of cell culture substrates

Gelatin-coated substrates were prepared by incubating tissue culture plates with 0.1% gelatin for 30 min. Fibrillar ECM was prepared from NIH-3T3 mouse fibroblasts using an established protocol (Mao and Schwarzbauer, 2005). Briefly, 2×10^4 fibroblasts/cm^2 were grown in fibroblast growth medium, supplemented with either 50 µg/ml unlabeled human FN or 45 µg/ml unlabeled human FN and 5 µg/ml FRET-FN for 6 days. 50 µg/ml mouse laminin-111 (Southern Biotech) was added to the fibroblast culture medium when indicated. After 6 days, fibroblast cultures were washed with PBS, wash buffer I (2 mM magnesium chloride, 2 mM EGTA, 100 mM sodium phosphate, pH 9.6), incubated at 37°C for 15 min in lysis buffer (8 mM sodium phosphate, 1% NP-40, pH 9.6) and replaced with fresh lysis buffer for an additional 60 min before final washes with wash buffer II (10 mM sodium phosphate, 300 mM potassium chloride, pH 7.5), PBS and sterile water.

Immunofluorescence staining

Cell cultures that underwent immunofluorescence staining were fixed with 3.7% formaldehyde for 20 min at room temperature. The cells were then incubated in a solution of 0.1% Triton X-100 and 5% goat serum in PBS for 30 min to permeabilize the cells and block non-specific binding. Samples were stained using AF1924 goat anti-SOX17 polyclonal antibody (1:100; R&D Systems), D27F4 rabbit anti-phospho-SMAD2 (1:200; Cell Signaling) and the appropriate Alexa-Fluor-dye-conjugated goat IgG or donkey IgG antibody (1:500). Cells were additionally labeled with Hoechst 33342 (1:2000) stain as indicated. Samples were examined on either a CARV or CARV II confocal microscope (BD Biosciences) mounted on a Nikon Eclipse TE2000-U microscope with IP Lab software or Nikon Ti-S microscope with Metamorph 7.6 software.

Quantitative PCR

RNA was extracted from ESCs by Trizol-chloroform extraction according to the manufacturer's instructions (Thermo Scientific) and cDNA was prepared from 2 µg of RNA. The quantitative PCR was performed (45 cycles, 95°C for 15 seconds followed by 60°C for 1 min) using a Bio-Rad CFX384 Real-Time System with the primer sets described in supplementary material Table S1, and the iQ SYBR Green Supermix. Data were analyzed by calculating quantities of RNA based on a standard curve generated from a fibronectin plasmid. GAPDH was used to normalize data, which was plotted as a fold change from that in undifferentiated mouse ESCs.

Deoxycholate-solubility assay

A deoxycholate (DOC)-solubility assay was used to separate cell lysates from DOC-insoluble ECM for western blot analysis, as described previously (Wierzbicka-Patynowski et al., 2004). Cultured cells were washed with PBS and lysed with DOC lysis buffer (2% sodium deoxycholate, 20 mM Tris-HCl, 2 mM EDTA, 2 mM PMSF, pH 8.8). The cell lysate was passed through a 27-G needle to reduce sample viscosity. The DOC-insoluble fraction was isolated by micro-centrifugation at 18,400 ***g*** for 20 min. The supernatant (cell lysate fraction) was removed; the DOC-insoluble fraction was then washed once with fresh DOC lysis buffer and resuspended in SDS-solubilization buffer (4% SDS, 20 mM Tris-HCl, 2 mM EDTA, 2mM PMSF, pH 8.8).

Western blotting

Cells were lysed using mRIPA buffer (Wierzbicka-Patynowski et al., 2007) or underwent a DOC-solubility assay (Wierzbicka-Patynowski et al., 2004), as described above. The protein concentrations of the samples were determined using a Pierce BCA Protein Assay kit (Thermo Scientific), according to the manufacturer's instructions. Equal protein amounts from each sample were separated by electrophoresis under reducing and denaturing conditions, transferred onto a nitrocellulose membrane and immunoblotted using ab40759 rabbit anti-SMAD4 monoclonal antibody (1:10^3; Abcam), ab8245 mouse anti-GAPDH monoclonal antibody (1:10^4; Abcam), ab76498 rabbit anti-SMAD7 antibody (1:10^3; Abcam), D27F4 rabbit anti-phospho-SMAD2 (1:10^3; Cell Signaling), D7G7 rabbit anti-SMAD2 (1:10^3; Cell Signaling), R457 rabbit anti-fibronectin polyclonal antiserum [1:2000; (Aguirre et al., 1994)], or ab11575 rabbit anti-laminin-111 polyclonal antibody (1:1000; raised against laminin from EHS basement membrane; Abcam) and the appropriate horseradish-peroxidase-conjugated goat or donkey IgG (1:10^4). Western blots were developed with ECL substrate (Pierce) and the integrated densities of bands within the linear range of the film were analyzed using Image J.

FACS

R1 ESCs grown for 5 days in definitive endoderm induction medium and the indicated integrin function-blocking antibody were analyzed by flow cytometry for their expression of the indicated laminin-binding integrin. After washing in PBS, R1s were detached using a 5-min treatment of TrypLE. Cells were then incubated for 30 min at 4°C in FACS buffer (2.5% donkey serum, 1 mM EDTA, 1% sodium azide in PBS) containing either 5 µg/ml GoH3 rat anti-α6-integrin or 5 µg/ml Ralph 3.1 mouse anti-α3-integrin antibody. After washing in FACS buffer, the R1s were incubated for 30 min at 4°C in FACS buffer containing 5 µg/ml of the appropriate Alexa-dye-conjugated goat or donkey IgG. R1s were centrifuged at 400 ***g*** for 5 minutes and washed in FACS buffer before being resuspended for analysis in a FACScan cytometer (Becton Dickinson). Fluorescence was measured at 488 nm and data were gated by size to measure single cells.

Statistical analysis

Statistical analyses were completed using Prism 5 (GraphPad Software, Inc.). Unpaired Student's *t*-tests were used when comparing two groups. Differences among three or more groups were assessed by ANOVA with Tukey's post hoc analysis to identify statistical differences as $P<0.05$. All data are presented as mean±s.e.m. Experimental data are shown for experiments performed in triplicate.

Acknowledgements

The authors thank Dr Michael Smith for providing a Matlab script used to analyze the FRET-FN images. The authors also thank Drs Jamie Kasuboski and James Fitzpatrick at the Waitt Advanced Biophotonics Center at the Salk Institute [supported by NCI P30 Cancer Center Support Grant CA014195-50 and NINDS P30 Neuroscience Center Core Grant NS072031-03A1 and by the W. M. Keck Foundation] for technical assistance with microscopy.

Competing interests
The authors declare no competing or financial interests.

Author contributions
H.T.-W. and A.J.E. contributed to the design of experiments. H.T.-W. and N.R. performed all experiments and data analysis. All authors contributed to the interpretation of data. H.T.-W. and A.J.E. wrote the manuscript.

Funding
This work was supported by grants from the National Institutes of Health [grant numbers NIH DP02OD006460 and NIH R21EB011727 to A.J.E.]. Pre-doctoral fellowship support was also provided by a National Science Foundation Graduate Research Fellowship (to H.T.-W.). Deposited in PMC for release after 12 months.

Supplementary material
Supplementary material available online at
http://jcs.biologists.org/lookup/suppl/doi:10.1242/jcs.166157/-/DC1

References

Aguirre, K. M., McCormick, R. J. and Schwarzbauer, J. E. (1994). Fibronectin self-association is mediated by complementary sites within the amino-terminal one-third of the molecule. *J. Biol. Chem.* **269**, 27863-27868.
Aumailley, M., Timpl, R. and Sonnenberg, A. (1990). Antibody to integrin α6 subunit specifically inhibits cell-binding to laminin fragment 8. *Exp. Cell Res.* **188**, 55-60.
Baneyx, G., Baugh, L. and Vogel, V. (2001). Coexisting conformations of fibronectin in cell culture imaged using fluorescence resonance energy transfer. *Proc. Natl. Acad. Sci. USA* **98**, 14464-14468.
Boo, S. and Dagnino, L. (2013). Integrins as modulators of transforming growth factor beta signaling in dermal fibroblasts during skin regeneration after injury. *Adv. Wound Care (New Rochelle)* **2**, 238-246.
Brafman, D. A., Phung, C., Kumar, N. and Willert, K. (2013). Regulation of endodermal differentiation of human embryonic stem cells through integrin-ECM interactions. *Cell Death Differ.* **20**, 369-381.
Chen, L. B., Murray, A., Segal, R. A., Bushnell, A. and Walsh, M. L. (1978). Studies on intercellular LETS glycoprotein matrices. *Cell* **14**, 377-391.
Chowdhury, F., Li, Y., Poh, Y.-C., Yokohama-Tamaki, T., Wang, N. and Tanaka, T. S. (2010a). Soft substrates promote homogeneous self-renewal of embryonic stem cells via downregulating cell-matrix tractions. *PLoS ONE* **5**, e15655.
Chowdhury, F., Na, S., Li, D., Poh, Y.-C., Tanaka, T. S., Wang, F. and Wang, N. (2010b). Material properties of the cell dictate stress-induced spreading and differentiation in embryonic stem cells. *Nat. Mater.* **9**, 82-88.
D'Amour, K. A., Agulnick, A. D., Eliazer, S., Kelly, O. G., Kroon, E. and Baetge, E. E. (2005). Efficient differentiation of human embryonic stem cells to definitive endoderm. *Nat. Biotechnol.* **23**, 1534-1541.
Darribère, T. and Schwarzbauer, J. E. (2000). Fibronectin matrix composition and organization can regulate cell migration during amphibian development. *Mech. Dev.* **92**, 239-250.
DeFreitas, M. F., Yoshida, C. K., Frazier, W. A., Mendrick, D. L., Kypta, R. M. and Reichardt, L. F. (1995). Identification of integrin α3β1 as a neuronal thrombospondin receptor mediating neurite outgrowth. *Neuron* **15**, 333-343.
Demyanenko, G. P., Schachner, M., Anton, E., Schmid, R., Feng, G., Sanes, J. and Maness, P. F. (2004). Close homolog of L1 modulates area-specific neuronal positioning and dendrite orientation in the cerebral cortex. *Neuron* **44**, 423-437.
DeQuach, J. A., Yuan, S. H., Goldstein, L. S. and Christman, K. L. (2011). Decellularized porcine brain matrix for cell culture and tissue engineering scaffolds. *Tissue Eng. A* **17**, 2583-2592.
Fu, J., Wang, Y.-K., Yang, M. T., Desai, R. A., Yu, X., Liu, Z. and Chen, C. S. (2010). Mechanical regulation of cell function with geometrically modulated elastomeric substrates. *Nat. Methods* **7**, 733-736.
Guvendiren, M. and Burdick, J. A. (2012). Stiffening hydrogels to probe short- and long-term cellular responses to dynamic mechanics. *Nat. Commun.* **3**, 792.
Higuchi, Y., Shiraki, N., Yamane, K., Qin, Z., Mochitate, K., Araki, K., Senokuchi, T., Yamagata, K., Hara, M., Kume, K. et al. (2010). Synthesized basement membranes direct the differentiation of mouse embryonic stem cells into pancreatic lineages. *J. Cell Sci.* **123**, 2733-2742.
Hodivala-Dilke, K. M., DiPersio, C. M., Kreidberg, J. A. and Hynes, R. O. (1998). Novel roles for α3β1 integrin as a regulator of cytoskeletal assembly and as a trans-dominant inhibitor of integrin receptor function in mouse keratinocytes. *J. Cell Biol.* **142**, 1357-1369.
Holle, A. W. and Engler, A. J. (2011). More than a feeling: discovering, understanding, and influencing mechanosensing pathways. *Curr. Opin. Biotechnol.* **22**, 648-654.
Holle, A. W., Tang, X., Vijayraghavan, D., Vincent, L. G., Fuhrmann, A., Choi, Y. S., del Álamo, J. C. and Engler, A. J. (2013). In situ mechanotransduction via vinculin regulates stem cell differentiation. *Stem Cells* **31**, 2467-2477.
Keller, R. (2005). Cell migration during gastrulation. *Curr. Opin. Cell Biol.* **17**, 533-541.
Kemler, R., Hierholzer, A., Kanzler, B., Kuppig, S., Hansen, K., Taketo, M. M., de Vries, W. N., Knowles, B. B. and Solter, D. (2004). Stabilization of beta-catenin in the mouse zygote leads to premature epithelial-mesenchymal transition in the epiblast. *Development* **131**, 5817-5824.
Khetan, S., Guvendiren, M., Legant, W. R., Cohen, D. M., Chen, C. S. and Burdick, J. A. (2013). Degradation-mediated cellular traction directs stem cell fate in covalently crosslinked three-dimensional hydrogels. *Nat. Mater.* **12**, 458-465.
Li, S., Edgar, D., Fässler, R., Wadsworth, W. and Yurchenco, P. D. (2003). The role of laminin in embryonic cell polarization and tissue organization. *Dev. Cell* **4**, 613-624.
Li, D., Zhou, J., Chowdhury, F., Cheng, J., Wang, N. and Wang, F. (2011). Role of mechanical factors in fate decisions of stem cells. *Regen. Med.* **6**, 229-240.
Liu, J., He, X., Corbett, S. A., Lowry, S. F., Graham, A. M., Fässler, R. and Li, S. (2009). Integrins are required for the differentiation of visceral endoderm. *J. Cell Sci.* **122**, 233-242.
Mao, Y. and Schwarzbauer, J. E. (2005). Stimulatory effects of a three-dimensional microenvironment on cell-mediated fibronectin fibrillogenesis. *J. Cell Sci.* **118**, 4427-4436.
Murry, C. E. and Keller, G. (2008). Differentiation of embryonic stem cells to clinically relevant populations: lessons from embryonic development. *Cell* **132**, 661-680.
Na, S., Collin, O., Chowdhury, F., Tay, B., Ouyang, M., Wang, Y. and Wang, N. (2008). Rapid signal transduction in living cells is a unique feature of mechanotransduction. *Proc. Natl. Acad. Sci. USA* **105**, 6626-6631.
Nagy, A., Rossant, J., Nagy, R., Abramow-Newerly, W. and Roder, J. C. (1993). Derivation of completely cell culture-derived mice from early-passage embryonic stem cells. *Proc. Natl. Acad. Sci. USA* **90**, 8424-8428.
Nakao, A., Afrakhte, M., Morén, A., Nakayama, T., Christian, J. L., Heuchel, R., Itoh, S., Kawabata, M., Heldin, N. E., Heldin, C. H. et al. (1997). Identification of Smad7, a TGFbeta-inducible antagonist of TGF-beta signalling. *Nature* **389**, 631-635.
Pajerowski, J. D., Dahl, K. N., Zhong, F. L., Sammak, P. J. and Discher, D. E. (2007). Physical plasticity of the nucleus in stem cell differentiation. *Proc. Natl. Acad. Sci. USA* **104**, 15619-15624.
Poh, Y.-C., Na, S., Chowdhury, F., Ouyang, M., Wang, Y. and Wang, N. (2009). Rapid activation of Rac GTPase in living cells by force is independent of Src. *PLoS ONE* **4**, e7886.
Reynolds, L. E., Conti, F. J., Silva, R., Robinson, S. D., Iyer, V., Rudling, R., Cross, B., Nye, E., Hart, I. R., Dipersio, C. M. et al. (2008). alpha3beta1 integrin-controlled Smad7 regulates reepithelialization during wound healing in mice. *J. Clin. Invest.* **118**, 965-974.
Robertson, E., Bradley, A., Kuehn, M. and Evans, M. (1986). Germ-line transmission of genes introduced into cultured pluripotential cells by retroviral vector. *Nature* **323**, 445-448.
Rognoni, E., Widmaier, M., Jakobson, M., Ruppert, R., Ussar, S., Katsougkri, D., Böttcher, R. T., Lai-Cheong, J. E., Rifkin, D. B., McGrath, J. A. et al. (2014). Kindlin-1 controls Wnt and TGF-β availability to regulate cutaneous stem cell proliferation. *Nat. Med.* **20**, 350-359.
Sheppard, D. (2000). In vivo functions of integrins: lessons from null mutations in mice. *Matrix Biol.* **19**, 203-209.
Skoglund, P., Rolo, A., Chen, X., Gumbiner, B. M. and Keller, R. (2008). Convergence and extension at gastrulation require a myosin IIB-dependent cortical actin network. *Development* **135**, 2435-2444.
Smith, M. L., Gourdon, D., Little, W. C., Kubow, K. E., Eguiluz, R. A., Luna-Morris, S. and Vogel, V. (2007). Force-induced unfolding of fibronectin in the extracellular matrix of living cells. *PLoS Biol.* **5**, e268.
Swift, J., Ivanovska, I. and Buxboim, A. (2013). Nuclear Lamin-A scales with tissue stiffness and enhances matrix-directed differentiation. *Science* **341**, 1-33.
Taylor-Weiner, H., Schwarzbauer, J. E. and Engler, A. J. (2013). Defined extracellular matrix components are necessary for definitive endoderm induction. *Stem Cells* **31**, 2084-2094.
Thiery, J. P. and Sleeman, J. P. (2006). Complex networks orchestrate epithelial-mesenchymal transitions. *Nat. Rev. Mol. Cell Biol.* **7**, 131-142.
Wartiovaara, J., Leivo, I., Virtanen, I., Vaheri, A. and Graham, C. F. (1978). Appearance of fibronectin during differentiation of mouse teratocarcinoma in vitro. *Nature* **272**, 355-356.
Wen, J. H., Vincent, L. G., Fuhrmann, A., Choi, Y. S., Hribar, K. C., Taylor-Weiner, H., Chen, S. and Engler, A. J. (2014). Interplay of matrix stiffness and protein tethering in stem cell differentiation. *Nat. Mater.* **13**, 979-987.
Wierzbicka-Patynowski, I., Mao, Y. and Schwarzbauer, J. E. (2004). Analysis of fibronectin matrix assembly. *Curr. Protoc. Cell Biol.* **25**, 10.12.1-10.12.10.
Wierzbicka-Patynowski, I., Mao, Y. and Schwarzbauer, J. E. (2007). Continuous requirement for pp60-Src and phospho-paxillin during fibronectin matrix assembly by transformed cells. *J. Cell. Physiol.* **210**, 750-756.
Yasunaga, M., Tada, S., Torikai-Nishikawa, S., Nakano, Y., Okada, M., Jakt, L. M., Nishikawa, S., Chiba, T., Era, T. and Nishikawa, S. (2005). Induction and monitoring of definitive and visceral endoderm differentiation of mouse ES cells. *Nat. Biotechnol.* **23**, 1542-1550.
Young, J. L. and Engler, A. J. (2011). Hydrogels with time-dependent material properties enhance cardiomyocyte differentiation in vitro. *Biomaterials* **32**, 1002-1009.